metric measurements using a Pt electrode also support the conclusion that adsorbed anion radical is present: simulations of the voltammogram are best fitted to the experimental curves when adsorption of the product of electron transfer is considered.

The differential reflectance spectrum recorded during the reduction of tetracyanoethylene (TCNE) in acetonitrile at a platinum electrode is shown in Figure 4. The positive bands due to disappearance of the TCNE substrate at the more negative potential are not visible. This is because the sensitivity of the transmission scale has been decreased to accomodate the full amplitude of the bands at 2187 and 2148 cm^{-1}. The band at 2148 cm^{-1} is almost 10^4 times larger than is predicted from a simple Beer's law calculation for the total amount of TCNE anion that has been found during the potential step. The weaker band at 2187 cm^{-1} corresponds closely to an assignment made by Devlin et al. to the C≡N stretch, which has been charge transfer enhanced by formation of a complex between the anion radical and a surface platinum atom. The stronger band increases markedly with an increase in the cell thin-layer gap and is therefore due to solution free C≡N fundamental stretch, enhanced most likely by the formation of an electron donor–acceptor complex between the anion radical and neutral TCNE. The point is under investigation.

Conclusions

The technique described is a very powerful new method for the rapid recording of the spectra of radical ion intermediates produced during electrochemical reactions. The method is capable of detecting spectra from short-lived species that could not otherwise be obtained.

Acknowledgment. Part of this work was supported by the Office of Naval Research.

Registry No. Platinum, 7440-06-4.

Electrochemical Stability of Catechols with a Pyrene Side Chain Strongly Adsorbed on Graphite Electrodes for Catalytic Oxidation of Dihydronicotinamide Adenine Dinucleotide

Hans Jaegfeldt,*† Theodore Kuwana,† and Gillis Johansson‡

Contribution from the Department of Chemistry, The Ohio State University, Columbus, Ohio 43210, and Analytical Chemistry, University of Lund, Lund, Sweden.
Received March 11, 1982

Abstract: The electrochemical stability and reactivity of 4-[2-(1-pyrenyl)vinyl]catechol (PSCH2) and 4-[2-(1-pyrenyl)-ethano]catechol (PECH2) strongly adsorbed on graphite electrodes were investigated as a function of the applied potential at pH 7.0. The surface coverage of these compounds ranged from 0.1×10^{-9} to 2.7×10^{-9} mol/cm^2. The "modified" electrodes exhibited deactivation which could be explained by second-order reactions between the catechols and the electrochemically produced quinones coupled with a second-order reaction between the quinones. The ethano compound showed a much larger decay rate, probably because of free rotation around the saturated bond connecting the pyrene part and the catechol group. The deactivation was apparently not associated with desorption of the compounds. The catechols in the oxidized form could *catalytically* oxidize NADH. The overpotential for NADH oxidation was thus decreased from 410 to 150 mV vs. SCE at pH 7.0. However, the catalytic current was found to decrease exponentially with increasing number of scans. The rate of this deactivation of the catalytic electrode was found to be inversely proportional to the coverage of immobilized mediator. The deactivation could be explained by a chemical coupling reaction between the mediator and NADH, forming a complex which gradually blocked off the surface of the electrode. The probable nature of the complex makes it unlikely that "capping" of active sites, e.g., the 2, 5, and 6 positions, on the catechol ring would effectively prevent the blocking and, hence, deactivation of the catalytic electrodes.

Introduction

The coenzyme nicotinamide adenine dinucleotide (NADH) is oxidized directly at different electrode materials only with high overvoltages.[1] The overvoltage at pH 7 is about 1.1 V at a carbon[2] and 1.3 V at a platinum electrode.[3] Attempts have been made to link the electrochemical oxidation of the coenzyme to the analysis of substrates for clinical purposes.[4,5] About 300 dehydrogenases are known which are dependent on NADH or NADPH as redox transfer agents. Electrodes modified to oxidize NADH more easily should therefore open up new applications both in analysis and in biotechnology.

Surface modifications have been proposed as a means of reducing the overvoltage of the electrochemical oxidation of NADH. Blaedel and Jenkins[6] reduced the overvoltage with 0.2 to 0.45 V vs. SCE with an electrochemical pretreatment of the electrode. They assumed that hydroxyl, carbonyl, and quinone groups produced by the oxidative pretreatment of the electrode caused this decrease of overvoltage. It has been shown in this laboratory that a catalytic electrode could be produced by the separate covalent attachment of 1,2-hydroquinones to the surface of pyrolytic graphite.[7] That work demonstrated the possibility of producing catalytic electrodes by the covalent incorporation of electron-transfer mediating groups onto the surface of the electrode. Recently, Degrand and Miller[8] modified a vitreous carbon

* Permanent address: Analytical Chemistry, University of Lund, P.O. Box 740, S-220 07 Lund, Sweden.
† The Ohio State University.
‡ University of Lund.

(1) Elving, P. J.; Schmakel, C. O.; Santhanam, K. S. V. *Crit. Rev. Anal. Chem.* **1976**, *6*, 1–67.
(2) Moiroux, J.; Elving, P. J. *Anal. Chem.* **1978**, *50*, 1056–62.
(3) Jaegfeldt, H. *J. Electroanal. Chem.* **1980**, *110*, 295–302.
(4) Blaedel, W. J.; Jenkins, R. A. *Anal. Chem.* **1976**, *48*, 1240–47.
(5) Thomas, L.C.; Christian, D. *Anal. Chim. Acta* **1978**, *78*, 271–76.
(6) Blaedel, W. J.; Jenkins, R. A. *Anal. Chem.* **1975**, *47*, 1337–43.
(7) Tse, D.C.S.; Kuwana, T. *Anal. Chem.* **1978**, *50*, 1315–18.
(8) Degrand, C.; Miller, L. L. *J. Am. Chem. Soc.* **1980**, *102*, 5728–32. Fukui, M.; Kitani, A.; Degrand, C.; Miller, L.L. *Ibid.* **1982**, *104*, 28–33.

0002-7863/83/1505-1805$01.50/0

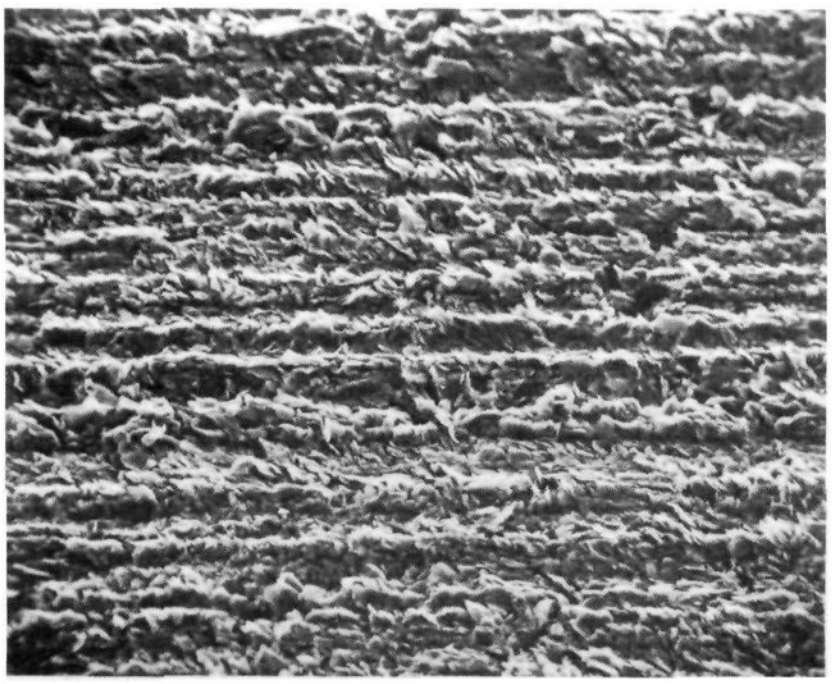

Figure 1. A picture of an emery-paper polished electrode taken with a scanning electron microscope reveals that the structure of the surface is quite complex, but still highly ordered. Besides the parallel grooves (arising from the polishing procedure) separated by a mean distance of approximately 10 μm, the surface is seen to consist of a large number of stacked parallel flakes. Magnification ×560; tilt 37°.

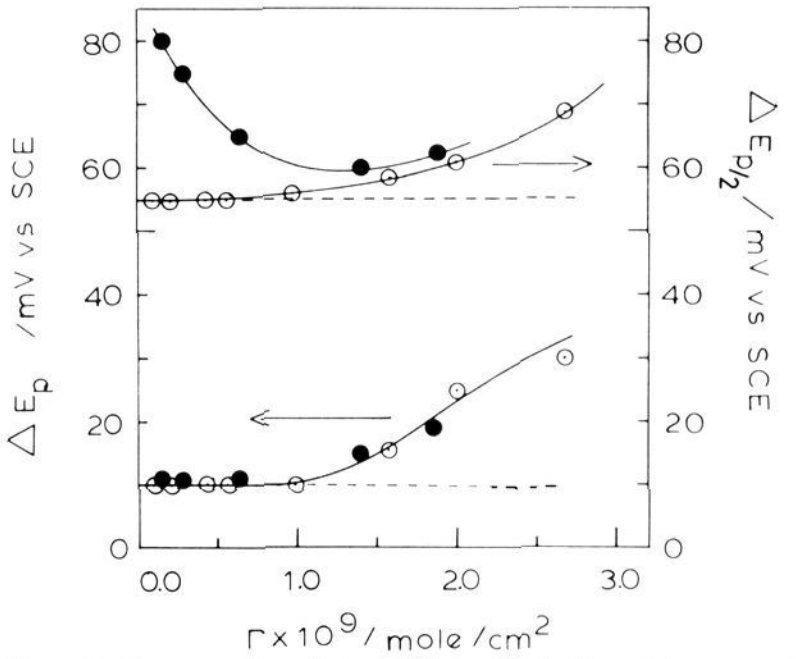

Figure 2. The separation of the anodic and cathodic peaks, ΔE_p, and the width at half-peak height, $\Delta E_{p/2}$, are shown as a function of surface coverage. The unfilled circles are before NADH oxidation and the filled ones after NADH oxidation. Both parameters are seen to be independent of the coverage below 1×10^{-9} mol/cm^2, but start to increase at higher coverages. The data points for a coverage of 1.58×10^{-9} mol/cm^2 were taken separately from the others which were also used for NADH oxidations. The scan rate was 50 mV/s; pH 7.0.

electrode with a polymer coating, to which dopamine was chemically bound, and showed that such electrodes were catalytically active for a number of cycles. The decrease of overvoltage was about 0.25 V.

It has been observed that polycyclic aromatic compounds adsorb strongly on graphite surfaces. The adsorption increases in strength with an increasing number of aromatic rings.[9-12] Since it is known that some 1,2-quinones are mediators in homogeneous solutions and also when covalently bonded to a surface,[7] there was a possibility that adsorbed 1,2-quinones might also mediate the electron transfer from NADH to the electrode. No such effect could be seen for 1,2-naphthoquinone, alizarin, phenanthrenequinone, or a number of other condensed aromatic quinones studied previously.[13] The adsorbed quinone functionality, which probably lies flat on the surface, seems to be in an unfavorable position for electron exchange with NADH. In an earlier report[14] a molecule which had a catechol group attached via a double bond to a naphthalene ring system was synthesized and studied. The small movement of the catechol group about the rigid double bond was found to be sufficient to facilitate fast electron exchange with NADH. However, the lifetime of the electrodes seemed to be limited by a relatively fast desorption of the compound.

This paper describes two types of compounds in which the naphthalene used previously was replaced with a pyrene ring system. The adsorption of this species on the electrode surface should be much stronger, since the number of aromatic rings is doubled. The solubility in aqueous solutions is also much less. This adsorbed layer should be much more stable toward desorption and, hence, should provide increased electrode stability if no other deactivating process exists.

Results and Discussion

Adsorbing Surface Area. Figure 1 shows a scanning electron microscope (SEM) picture of an emery paper polished surface of the spectrographic graphite electrode. Many parallel grooves are visible with a mean separation of approximately 10 μm. In addition to these grooves from the polishing procedure, it can be seen that the surface consists of stacked flakes of differing sizes. It is obvious that the surface area available for adsorption is much greater than the geometrical one. A calculation of the area available for adsorption is quite difficult, but the number of flakes per unit area and their mean size yields a real area estimate of two to five times the geometrical one. As mentioned in the Experimental Section (vide infra), the electrochemical surface area seen by a diffusing species in solution is equal to the geometrical area. This is reasonable since the diffusion layer always extends into the solution more than the electrode topography. Lack of knowledge of the exact adsorbing electrode area is a complication, but this drawback is outweighed by the material's propensity for adsorption. Actually, a surface area greater than the geometric one is an advantage when the electrochemical catalysis process proceeds through an EC mechanism. This is realized when surface coverage per adsorbing real area of a catalyst is considered. In the case where only a moderate surface coverage is achieved, the resulting projection of that coverage upon a plane at the surface of the electrode, as seen from the solution by a diffusing species, may be many times greater, depending on the roughness of the electrode. Hence, a high catalytic current may be achieved although the actual surface coverage may be low.

Number of Layers. The cross-sectional area of a $PSCH_2$ molecule (A) when adsorbed flat on the surface is calculated, using

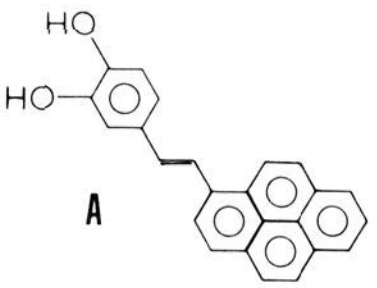

A

the geometric area, to be 0.6×10^{-14} cm^2. For the electrode with the lowest surface coverage attained, 0.10×10^{-9} mol/cm^2, this would correspond to one-third of a monolayer, and for the highest coverage of 2.7×10^{-9} mol/cm^2, the coverage would be almost 10 monolayers. The previous discussion about the dimension of the adsorbing surface area of this electrode material obviously means that the actual surface coverages are much lower.

Figure 2 shows how two electrochemical parameters for the adsorbed PSHC2 molecule vary with coverage. The separation of the peaks, ΔE_p, a measure of the apparent electrochemical rate constant,[15] is seen to remain constant at 10 mV for a scan rate of 50 mV/s up to a coverage of 1×10^{-9} mol/cm^2. A maximum

(9) Brown, A. P.; Koval, C.; Anson, F. C. *J. Electroanal. Chem.* **1976**, *72*, 379–87.
(10) Brown, A. P.; Anson, F. C. *Anal. Chem.* **1977**, *49*, 1589–95.
(11) Brown, A. P.; Anson, F. C.; *J. Electroanal. Chem.* **1977**, *83*, 203–6.
(12) Gorton, L.; Johansson, G. *J. Electroanal. Chem.* **1980**, *113*, 151–8.
(13) Gorton, L.; Torstensson, A., University of Lund, Sweden, unpublished work, 1980.
(14) Jaegfeldt, H.; Torstensson, A.; Gorton, L.; Johansson, G. *Anal. Chem.* **1981**, *53*, 1979–82.
(15) Laviron, E. *J. Electroanal. Chem.* **1979**, *101*, 19–28.

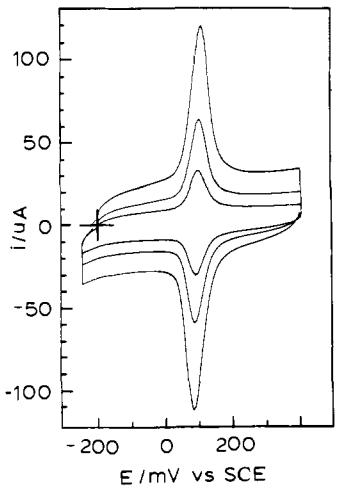

Figure 3. Cyclic voltammograms of PSCH2 adsorbed on the graphite electrode in a 0.10 M pyrophosphate buffer at pH 7.0, with a surface coverage of 0.95×10^{-9} mol/cm^2. The starting potential was −200 mV vs. SCE and scan rates were 25, 50, and 100 mV/s. $E^{0'}$ = +95 mV vs. SCE.

peak separation of 30 mV is reached for a coverage of 2.7×10^{-9} mol/cm^2. The small peak separation at low coverages is close to the theoretical value for an immobilized redox couple in equilibrium with the electrode potential.[16] The width at half-peak height, $\Delta E_{p/2}$, also stays virtually constant, at 55 mV, up to a coverage of 1×10^{-9} mol/cm^2. The effect of the increased coverage causes peak broadening which is not quite as abrupt, but still clear. It has been shown in a series of papers by Laviron and co-workers[15-18] that if there are interactions between molecules adsorbed on an electrode surface, these will affect the peak potentials and the peak widths. Therefore, the broadening of the peaks and the increasing peak potential shifts that begin around 1×10^{-9} mol/cm^2 strongly suggest that monolayer coverage has been reached at this value of coverage. A monolayer coverage of 1×10^{-9} mol/cm^2 corresponds to an adsorbing surface area of 0.84 cm^2, which is three times greater than the geometrical one. This factor is quite close to the one estimated from the number and size of the flakes. Experimental results from the catalytic oxidation of NADH also suggest that a monolayer is reached at this coverage. It is therefore concluded that the actual coverages attained in this work range from one-tenth of a monolayer up to ca. three monolayers.

Electrochemistry of Adsorbed PSCH2. Figure 3 shows cyclic voltammograms of a PSCH2-covered electrode obtained in a buffer solution with no NADH present. The peak current was found to increase linearly with scan rates from 25 to 200 mV/s. At 200 mV/s kinetic effects in the electron transfer rate begin to influence the linear relationship.[19] The apparent electrochemical rate constant was calculated to be 4 (±1) s^{-1} by measuring the separation of the peaks as a function of the scan rate between 25 and 600 mV/s for an electrode with a coverage of 0.90×10^{-9} mol/cm^2 at pH 7.0.[15] The width at half-peak height is 55 mV which is close to the theoretical value $90/n$ for a two-electron, two-proton electrochemical reaction involving an adsorbed species.[16] The number of electrons in the reaction, assuming a Nernstian response, was calculated from the equation:

$$i_p = [n^2F^2/4RT]A\Gamma_0 v \qquad (1)$$

where the parameters have their usual significance.[8,20] For an electrode with a coverage of 0.90×10^{-9} mol/cm^2, a plot of i_p/Q vs. v, where $Q = nFx$ and x is the number of moles, gave a value of n = 1.97 (±0.05) for scan rates lower than 50 mV/s. Higher scan rates yielded lower n values because of the influence of the electrochemical kinetics on the peak current (ref 17, Figure 3).

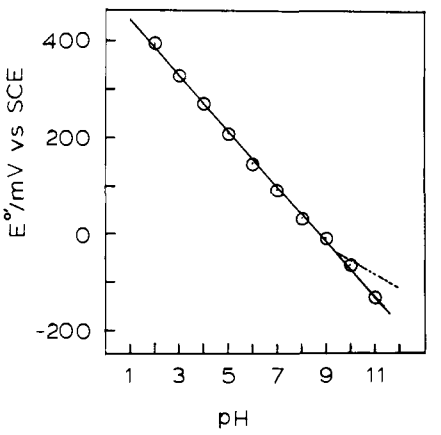

Figure 4. The $E^{0'}$ for the adsorbed PSCH2 was found to vary linearly between pH 2.0 and 11.0 with a slope of 58 mV/pH. Since the pK_a of pyrocatechol is 9.8, a change of slope would be expected at higher pH values (dotted line). The influence on the pK_a by the pyrene–stilbene side chain would be expected to decrease the pK_a owing to the stabilizing effect of the conjugated system on the deprotonated species.

Figure 4 shows $E^{0'}$ as a function of pH. The $E^{0'}$ was taken as the average value of the anodic and cathodic peak potentials at a scan rate of 25 mV/s, where no kinetic effects would adversely distort the peaks. The slope was found to be 58 mV/pH unit over a pH range from 2.0 to 11.0, as expected for a two-electron, two-proton electrochemical reaction. However, since the pK_a of a soluble catechol (pyrocatechol) is known to be 9.8,[21] a change of slope from 58 mV/pH to 29 mV/pH would be expected at higher pHs. In addition, a change in the pK_a by the aromatic substituent would be expected to give a lower value owing to the stabilizing effect of the conjugated system on the deprotonated species. Since no change in slope was observed, it has to be assumed that no deprotonation of the adsorbed PSCH2 is taking place at the expected pH. Changes in pK_a's of adsorbed species have previously been reported, for example, for FAD adsorbed on the same kind of electrode.[12,22]

Stability of Adsorbed PSCH2. The low solubility of PSCH2 in water and the strength of the adsorption onto the spectrographic graphite made the adsorbed layer very stable toward desorption. When an electrode with a coverage of 0.76×10^{-9} mol/cm^2 was washed with deionized water for 1 h, no loss of adsorbed species could be detected. Even a jet of methanol directed on the electrode surface for several minutes resulted in only a few per cent loss. These experiments were performed with the mediator in its reduced state. When the potential was scanned for extended periods of time, a slow decrease of the electroactive species was observed. After 5 h of scanning (710 scans) between −200 and +430 mV at pH 7.0, 65% of the original coverage of 0.93×10^{-9} mol/cm^2 remained. However, it was found that this loss of activity was not due to desorption but was caused by a potential dependent chemical reaction of the mediator on the electrode surface. A similar potential dependence of the stability has been observed previously in this laboratory[23] for catechols immobilized through covalent or polymeric attachment on glassy carbon electrode surfaces.

The potential dependence of the adsorbed layer was studied by applying a constant potential and then monitoring the electrochemically active mediator as a function of time. The amount of electrochemically active mediator was measured at discrete times by scanning the potential over the range required for one complete cyclic voltammogram. The scan rate was 100 mV/s,

(16) Laviron, E. *J. Electroanal. Chem.* **1974**, *52*, 395–402.
(17) Laviron, E. *J. Electroanal. Chem.* **1979**, *100*, 263–70.
(18) Laviron, E.; Roullier, R.; Degrand, C. *J. Electroanal. Chem.* **1980**, *112*, 11–23.
(19) Laviron, E.; Roullier, R. *J. Electroanal. Chem.* **1980**, *115*, 65–74.
(20) Bard, A. J.; Faulkner, L. R. "Electrochemical Methods, Fundamentals and Application"; Wiley: New York, 1980, p 522.
(21) "Handbook of Chemistry and Physics", 61st ed.; Chemical Rubber Co.: Cleveland, Ohio, 1980–81.
(22) Gorton, L., unpublished work, University of Lund, Sweden, 1980.
(23) Ueda, C.; Tse, D. C. S.; Kuwana, T. *Anal. Chem.* **1982**, *54*, 850–56.

and the total scan time was 12 s. Since the time scale for the whole experiment was on the order of 6 to 12 h, individual measurements of the coverage by cyclic voltammetry had a negligible influence on the measured decay rate. In order to ensure that the value of the acquired rate constant was unaffected even at the lowest decay rates, only a few scans were made. The experiments were performed at pH 7.0 using eight different electrodes at eight different settings of the potential. The coverage at $t = 0$ did not vary by more than ±15% from a mean value of 1.9×10^{-9} mol/cm^2. A plot of log (Γ/Γ_0) vs. time, where Γ is the coverage at any given time and Γ_0 is the coverage at $t = 0$, yielded a set of curves with an initial fast decay followed by a fairly linear segment.[23] At potentials lower than 0.0 V the rate of loss is virtually zero. When the potential is made more positive, the decay rate starts to increase, and when the potential is near $E^{0'} + 95$ mV at pH 7.0, a maximum is observed. When the potential is increased further, the decay rate levels off (Figure 6).

This observed potential dependence of the stability of the adsorbed layer has at least two aspects. Firstly, it could be argued that the quinone form of of the PSCH2 molecule could have a much higher rate of desorption than the hydroquinone form. However, the presence of a peak in Figure 6 does not support such an argument. Secondly, the simple first-order chemical process

$$QH_2 \underset{}{\overset{\text{rev.}}{\rightleftharpoons}} Q \xrightarrow{k_{obsd}} \text{products} \qquad \text{(I)}$$

proposed in the deactivation of a eugenol-modified electrode[23] cannot alone explain the observed behavior for the PSCH2 electrode. More complicated reaction paths must exist. Examples of surface reactions which could explain the observed behavior are given in reactions II and III, where QH_2 is the reduced species, Q· is the semiquinone, and Q is the quinone species.

$$QH_2 \overset{\text{rev.}}{\rightleftharpoons} Q\bullet \overset{\text{rev.}}{\rightleftharpoons} Q \xrightarrow{k_b} \text{products} \qquad \text{(II)}$$

$$Q\bullet \xrightarrow{k_a} \text{products}$$

$$QH_2 \overset{\text{rev.}}{\rightleftharpoons} Q \xrightarrow{k_b} \text{products} \qquad QH_2 + Q \xrightarrow{k_a} \text{products} \qquad \text{(III)}$$

If the lifetime of the semiquinone is sufficiently long, reaction II can account for the observed peak in Figure 6. However, the sharpness of the anodic and cathodic peaks and the fact than n was calculated as 2.0 indicate that this pathway may be less likely than the reactions in (III).

A solution of the differential equation (see Appendix)

$$-d\Gamma/dt = k_a[QH_2][Q] + k_b[Q]^2 \qquad (2)$$

describing the time-dependent loss of electroactive mediator for a second-order reaction between the hydroquinone and the quinone, coupled with a second-order reaction between the quinones, is:

$$\left(\frac{1}{\Gamma} - \frac{1}{\Gamma_0}\right) = (k_a B(E) + k_b)t/(1 + B(E))^2 \qquad (3)$$

where the rates of the reactions are k_a and k_b, and the equation

$$B(E) = [QH_2]/[Q] = \exp[(E^{0'} - E)2F/RT] \qquad (4)$$

gives the relative concentrations of the two species at different potentials. Figure 5 shows plots of $(1/\Gamma - 1/\Gamma_0)$ vs. time, t. These plots, all passing closely through the origin, affirm the proposed second-order nature of the decay mechanism. The potential dependence of the slopes in Figure 5 is shown in Figure 6. The trace in this figure is drawn using the equation

$$k_{exp} = (k_a B(E) + k_b)/(1 + B(E))^2 \qquad (5)$$

which is the "slope factor" in eq 3. A good fit between the experimental data points and the theoretically calculated solid trace in Figure 6 is obtained when $k_a \simeq 10 \times 10^5$ cm^2 mol^{-1} s^{-1} and $k_b \simeq 0.8 \times 10^5$ cm^2 mol^{-1} s^{-1}. Since the hydroquinone form

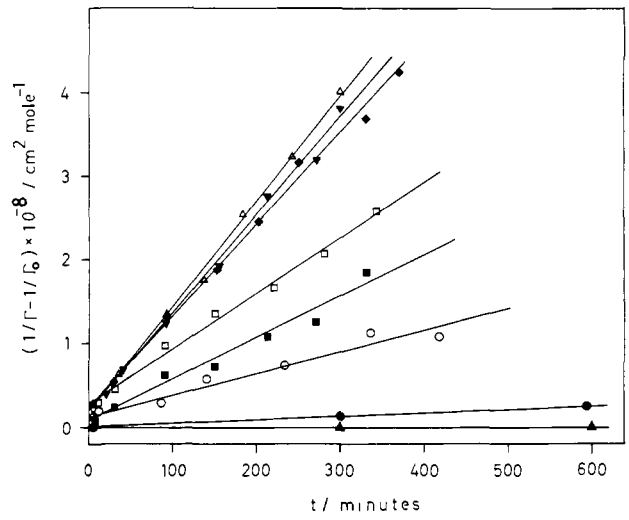

Figure 5. A second-order plot, i.e., $(1/\Gamma - 1/\Gamma_0)$ vs. time, for the decrease of the adsorbed electrochemically active $PSCH_2$ yields a set of straight lines with different slopes depending on the applied potentials: (▲) −100, (●) 0, (○) 50, (▼) 90, (△) 115, (♦) 135, (□) 200, and (■) 250 mV vs. SCE. The linearity of the plots as well as the potential dependence of the slopes (Figure 6) supports the proposed second-order chemical deactivation mechanism. See text for further details.

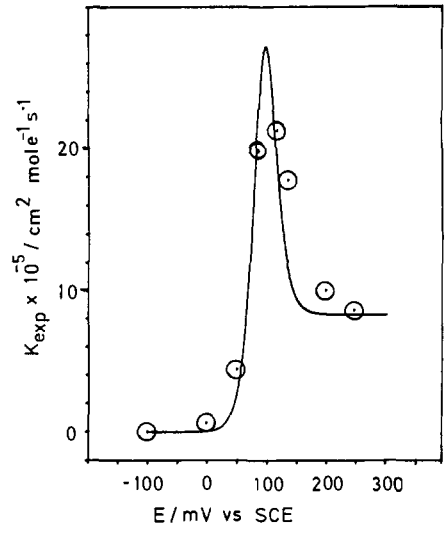

Figure 6. The figure shows a plot of the observed decay rate, k_{exp}, of electrochemical activity for adsorbed $PSCH_2$ at different potentials (Figure 5). The solid line is a theoretical curve usin $k_a = 10 \times 10^5$ cm^2 mol^{-1} s^{-1} and $k_b = 0.8 \times 10^5$ cm^2 mol^{-1} s^{-1}. See text for further details.

is a slightly better nucleophile than the quinone, the reaction rate k_a of the chemical reaction in (IV) would be expected to be

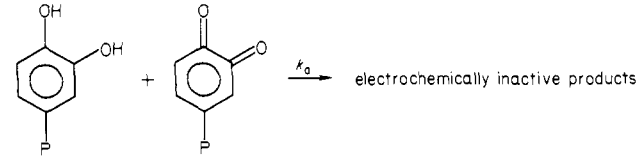

(IV)

somewhat faster than the rate k_b of reaction V. In both cases,

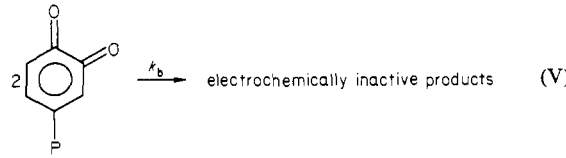

(V)

ether linkages and other unspecified polymeric forms may be produced, decreasing the concentration of electroactive catechols on the surface.[24] However, a curve derived from the radical

reaction II would fit just as well, assuming that the radical reaction is five times faster than the quinone one and that the $E^{0'}$'s of the two steps are equal. It is not possible from the acquired data to distinguish between these two models; both reactions may actually occur simutaneously.

Other reactions also occur. If the potential is scanned to +1.24 V, a large oxidation peak is seen as the background discharge becomes prominent. This peak is most likely due to the oxidation of the pyrene ring.[25] When the potential scan is reversed, the redox couple at +95 mV is no longer seen and a new one appears at −82 mV. This redox couple shows a pH dependence that can be ascribed to a two-electron, two-proton reaction. The stability of the new redox couple is independent of time and remains unaffected after several hours of scanning. The low $E^{0'}$ value and its inability to catalyze NADH makes it probable that the redox couple is formed through cyclization of the pyrene and catechol parts of the molecule (B). The dotted circle in structure B

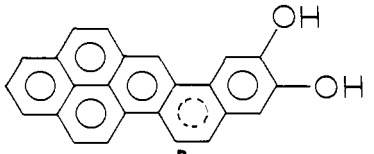

B

indicates a new six-membered ring, formed upon cyclization of compound A. The cation radical formed via oxidation of the pyrene ring[25] would make it possible for the molecule to cis–trans isomerize at the otherwise rigid double bond. The formation of a new redox couple is seen also for the PECH2-modified electrode. The yield of the new compound is not quantitative and seems to be a function of coverage.

Another "bound" mediator, 4-[2-(9-anthracenyl)vinyl]catechol, not further investigated in this work, showed the same disappearance of the redox couple after oxidation at +1.25 V, but no new redox couple was found at −82 mV. A probable reason is, for conformational reasons, that this species cannot form another six-membered ring through cyclization.

Electrochemistry of Adsorbed PECH2. Figure 7 shows cyclic voltammograms of a PECH2 (C) covered electrode, obtained in

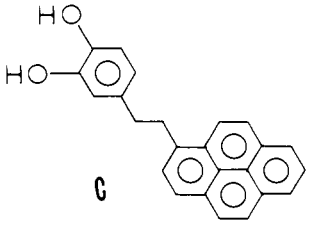

C

a PECH2-free buffer solution. The $E^{0'}$ is virtually the same as for the PSCH2-modified electrode. No significant difference in the $E^{0'}$ value would be expected with the change from a conjugated to an unconjugated "bridge" between the pyrene and the catechol ring.[26] The same dependence of $E^{0'}$ on pH is also found. However, the electroactive coverage decreases to 50% of the original in as few as 80 cycles, when scanned between −200 and +430 mV at 50 mV/s. The PSCH2-modified electrode scanned over the same potential range showed only a 5% decrease for the same number of scans. Experiments, in which the electrode was washed with deionized water and methanol showed results similar to those of the PSCH2-covered electrode. An analogous dependence of stability on the potential was also observed. However, since the rate of the electrochemical decay was so rapid, approximately the same as the time of a single scan, it was not possible to study the rate of loss of electroactive mediator at different potentials. It is estimated that there is a 10-fold decrease in stability compared to PSCH2. This very significant change

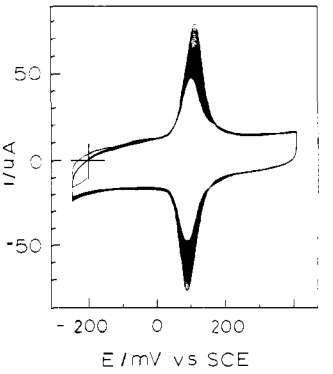

Figure 7. Cyclic voltammograms of PECH2 adsorbed on the graphite electrode in a 0.10 M pyrophosphate buffer at pH 7.0 with an orginal coverage of 1.5×10^{-9} mol/cm^2. The starting potential is −200 mV vs. SCE. The scan rate is 50 mV/s; $E^{0'}$ = +100 mV. A sharp decrease of the electroactivity is seen during the 80 scans shown. Under the same conditions a PSCH2 modified electrode lost only 5% of its electroactivity.

in stability must be caused by the presence of free rotation between the anchor part and the catechol in the PECH2 molecule. Therefore, the probability of reacting with a neighbor is much greater with PECH2 than for the PSCH2 molecule, in which the catechol is held in a plane by the rigid double bond. Although catalytic oxidation of NADH was observed, the immobilized mediator itself showed sufficient instability that further investigation of the PECH2-covered electrode was not undertaken.

Homogeneous Side Reaction of PSCH2. In early studies on the adsorption of FAD and several flavines on spectrographic graphite electrodes,[12,27] it was found that the electrochemical kinetics of the adsorbed species was much faster when HCl was added to the solution from which they were adsorbed. On the other hand, when PSCH2 was adsorbed from a MeOH/H_2O/HCl solution, only adverse effects were observed. After a few days in the acid solution a new redox couple started to appear on the cyclic voltammograms, and after 1 week at room temperature no PSCH2 was detected. The new redox couple showed a pH dependence of $E^{0'}$ identical with that of PECH2, but the rate of decay vs. the number of scans was much faster. In fact, the rate of decay was about the same order of magnitude as found for the PECH2-modified electrode discussed above. This strongly suggests that the new redox couple, formed slowly in MeOH/H_2O/HCl solution, is a species in which an addition to the double bond has occurred. Some of the species in the solution that could be responsible for such an addition are HCl, added to the double bond, and MeOH or water added by acid catalysis. Considering the positive change in the $E^{0'}$ value from +95 to +180 mV vs. SCE, a species formed from the HCl seems likely.[26] The electronegative chlorine atom would probably exert an electron-withdrawing effect on the catechol ring. The magnitude of the change in $E^{0'}$ is surprisingly large.[26] Further investigation of the exact nature of this new redox couple was not pursued since it showed lower stability and had a more positive $E^{0'}$ value which would be undesirable for NADH catalysis.

Catalytic Oxidation of NADH. Figure 8, curve A, shows a cyclic voltammogram obtained with a PSCH2-covered electrode in a 2.0 mM NADH solution at pH 7.0. There is a significant increase in the current at the potential where PSCH2 is oxidized, compared to the scan in the buffer solution without NADH, curve B. The cause of the increased current is that the NADH present in the solution diffuses toward the electrode and reduces the PSC produced electrochemically. The overall reaction proceeds according to an EC catalytic mechanism, eq 6–8:

$$\text{PSCH2} \rightarrow \text{PSC} + 2\text{H}^+ + 2\text{e}^- \quad (6)$$

$$\text{PSC} + \text{NADH} + \text{H}^+ \xrightarrow{k_1} \text{PSCH2} + \text{NAD}^+ \quad (7)$$

$$\text{net:} \quad \text{NADH} \rightarrow \text{NAD}^+ + \text{H}^+ + 2\text{e}^- \quad (8)$$

(24) Ryan, M. D.; Yuehm A.; Chen, W. Y. *J. Electrochem. Soc.* **1980**, *127*, 1489–95.
(25) Zweig, A.; Maurer, A. H.; Roberts, B. G. *J. Org. Chem.* **1967**, *32*, 1322–29.
(26) Horner, L.; Geyer, D. E. *Chem. Ber.* **1965**, *98*, 2016–45.
(27) Gorton, L. Doctoral Dissertation, Department of Analytical Chemistry, University of Lund, S-220 07 Lund, Sweden, 1981.

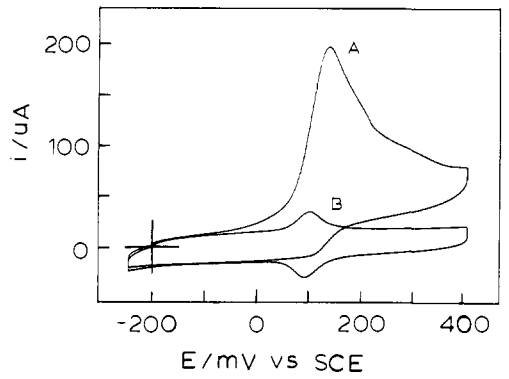

Figure 8. Catalytic oxidation of NADH mediated by adsorbed PSCH2 (curve A), 2.0 mM NADH, pH 7.0, scan rate 50 mV/s. Curve B shows a PSCH2 modified electrode in a buffer solution without NADH: coverage 0.4×10^{-9} mol/cm^2 and starting potential of −200 mV vs. SCE.

The rate-determining step is reaction 7, with a rate constant, K_1. The net electrode reaction is given by eq 8. The catalytic peak is found at +150 mV, compared to the uncatalyzed value at +410 mV.[14] Thus, a decrease in the overvoltage of 260 mV is observed.

The peak current, i_p, was found to vary only slightly with the coverage of the electrode for the first scan and followed quite closely the equation given by Andrieux and Saveant:[28]

$$i_p = 0.496nFA(D_R nFv/RT)^{1/2}C_R \quad (9)$$

For the two lowest coverages used, 0.10×10^{-9} and 0.21×10^{-9} mol/cm^2, slightly lower values than 0.496 were observed. From Figure 1 in the paper by Andrieux and Saveant, where a plot of the "constant" 0.496 is given as a function of

$$\log [K_1\Gamma/(D_R nFv/RT)^{1/2}] \quad (10)$$

the reaction rate constant, K_1, was calculated to be 1×10^4 M^{-1} s^{-1}. This is 10 times faster than that calculated previously[29] for a naphthalene–vinylcatechol adsorbed on a graphite surface.[14]

The homogeneous rate constants have been calculated previously for several catechols with different side chains.[7] The rate constants were found to vary from 4×10^2 to 8×10^4 M^{-1} s^{-1} for 1,2-naphthoquinone-4-sulfonic acid and 3,4-dihydroxybenzylamine, respectively, and to be a function of ΔG in a homogeneous solution.[7] On the other hand, 1,2-naphthoquinone showed no catalytic effect when adsorbed on a graphite electrode, in spite of an appreciable reaction rate in homogeneous solution. Therefore, the accessibility of the quinone group as well as the ΔG of the reaction must influence the heterogeneous reaction rate.

Catalytic Stability. Despite the high stability of the PSCH2-modified electrode in buffer solution with no NADH present, consecutive scans with this electrode in a 2.0 mM NADH solution resulted in a drop of the catalytic current. The catalytic stability was found to be dependent on the original coverage of mediator. Seven different electrodes, with coverages ranging from 0.10×10^{-9} to 2.7×10^{-9} mol/cm^2, were studied.

Figure 9 shows the decrease in the catalytic peak current expressed as a ratio of $i_{p,cat}/i_{p,cat,1st\ scan}$ vs. the number of scans. The electrodes with low coverages showed a much faster loss of catalytic activity than those with high coverages. For an electrode with a coverage of 0.10×10^{-9} mol/cm^2, only 50% of the catalytic current remained after five scans. The electrode with the highest coverage, 2.7×10^{-9} mol/cm^2, exhibited a much higher degree of stability and more than 90% of the catalytic current remained after 30 scans. The exponential character of the curves in figure 9 is verified by the linearity of the plots of the logarithm of $i_{p,cat}/i_{p,cat,1st\ scan}$ vs. the number of scans. A set of straight lines is obtained, with different slopes depending on the coverage, suggesting a first-order deactivation reaction. In fact, the solid curves drawn in Figure 9 are obtained from the regression analysis of the logarithmic plots. The decay follows the equation:

$$i_{p,cat} = i_{p,cat,1st\ scan} \times 10^{(-k(n-1))} \quad (11)$$

where k is the slope and n is the number of scans. An inverse relationship was found to exist between the slope constant, k, and the coverage, Γ. This is shown in Figure 10, where $1/k$ is plotted vs. Γ, giving a linear relationship for coverages below 1×10^{-9} mol/cm^2. However, a marked deviation from a linear dependence is observed for the two highest coverages. According to previous discussion, these coverages correspond to two or three monolayers. The deviation indicates that an apparently more stable catalytic electrode is produced per adsorbed mediator. This appears to be a side effect of the deactivation process, and will be discussed later.

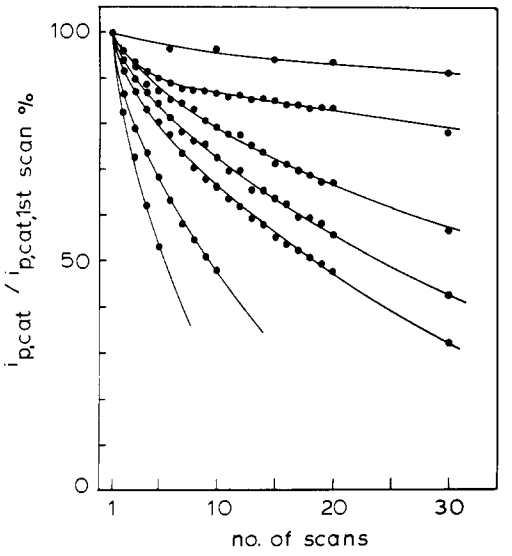

Figure 9. Plots of $i_{p,cal}/i_{p,cal,1sl\ scan}$ vs. the number of scans, in a 2.0 mM NADH solution containing 0.10 M pyrophosphate buffer at pH 7.0. The starting and switching potentials are −200 and +430 mV vs. SCE. The scan rate was 50 mV/s. The coverages are 0.10, 0.21, 0.43, 0.56, 0.95, 2.0, and 2.7×10^{-9} mol/cm^2. The lowest coverage produces the fastest rate of catalytic decay and the highest coverage the slowest. The entire experiment was performed in the same NADH solution for all the electrodes.

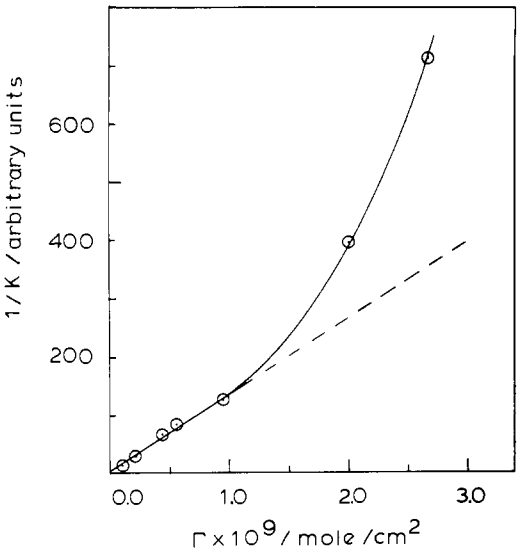

Figure 10. A plot of the log of $i_{p,cal}/i_{p,cal,1sl\ scan}$ vs. the number of scans, shows that the catalytic decay (Figure 9) follows the equation $Y = Y_0 \times 10^{(-k(n-1))}$. When the inverse of the slope in this equation (i.e., $1/k$) is plotted vs. the coverage of the electrode, a linear relation is found for coverages below 1×10^{-9} mol/cm^2. A relatively lower catalytic decay rate is observed for the two highest coverages, 2.0×10^{-9} and 2.7×10^{-9} mol/cm^2.

(28) Andrieux, C. P.; Saveant, J. J. *J. Electroanal. Chem.* **1978**, *93*, 163–68.

(29) An unfortunate misprint in ref 14 gave $K_1 = 2 \times 10^6$ instead of the correct value, 2×10^3 M^{-1} s^{-1}.

Table I[a]

electrode	θ_A $\times 10^9$/ mol	θ_B $\times 10^9$/ mol	$\Delta\theta$ $\times 10^9$/ mol	ΣNADH $\times 10^7$/ mol	ΣNADH/ $\Delta\theta$	no. of scans
1	0.028					5
2	0.0581	0.0303	0.0278	0.0304	1093	10
3	0.120	0.0405	0.0755	0.0855	1132	30
4	0.158	0.0776	0.0804	0.862	1072	30
5	0.267	0.180	0.0870	0.921	1059	30
6	0.564	0.391	0.173	1.13	653	30
7	0.751	0.527	0.224	1.17	522	30

[a] θ_A is the amount of electroactive mediator on the electrode before scanning in a 2.0 mM NADH solution from −200 to +430 mV vs. SCE. θ_B is the amount of electroactive mediator left after a number of catalytic scans; see last column. ΣNADH is the total amount of NADH oxidized over the total number of scans and ΣNADH/$\Delta\theta$ is the number of oxidized NADH molecules per deactivated mediator on the surface of the electrode.

Influence on the Mediator by the Catalysis. The adsorbed mediator was studied using cyclic voltammetry before and after the catalytic NADH oxidation experiments. The filled circles in Figure 2 show the peak shifts, ΔE_p, and the peak widths at half-peak height, $\Delta E_{p/2}$, as a function of the coverage after the catalytic oxidations. The peak separations seem to be a function only of the electrode coverage. This indicates that there has been no change in the electrochemical kinetics induced by the catalytic NADH oxidations.[16] The peak widths, however, show a marked change, giving much broader waves after catalysis (Figure 2). This effect increases with decreased coverages. The broadening of the waves suggests that stronger interactions between the adsorbed mediators occur after several catalytic scans have been made.[16]

The data in Table I show that a noticeable decrease in the electroactive mediator has taken place after the catalytic oxidations of NADH. This decrease may be due to either loss of mediator into the solution or deactivation of the adsorbed species. Table I also gives the total amount of oxidized NADH produced by each electrode, $\sum$NADH. The change in the coverage of the mediator, $\Delta\theta$, is also given. The ratio of $\sum$NADH/$\Delta\theta$ gives the total number of oxidized NADH molecules per inactivated or lost mediator. For coverages below 1×10^{-9} mol/cm^2, a constant value of $\sum$NADH/$\Delta\theta$ = 1090 (±30) is obtained. This shows that, on the average, 1100 NADH molecules can be oxidized by one adsorbed mediator, before a side reaction with NADH makes it electrochemically inactive.

Blocking Mechanism. Even though a decrease in the coverage of electroactive mediator is observed after successive scans in a NADH solution, the amount of mediator remaining on the electrode should be sufficient to maintain the catalytic current with very little decrease on the subsequent scan (see data in Table I). The fact that a decrease is actually observed suggests that a "blocking" of the available mediators left on the electrode is occurring. Adsorption of the product NAD^+ is ruled out as a blocking mechanism,[30] since experiments in which the electrode was dipped into a 2.0 mM NAD^+ solution for several minutes showed no adverse effects on the catalytic current. Thus, the experiments provide evidence that there is a chemical side reaction between the oxidized PSCH2 adsorbed on the electrode and the NADH in the solution, and that the reaction complex is, at most, only partly desorbed.

A mechanism explaining the experimental data for the catalytic behavior is proposed by the following model. The blocking is caused by a reaction between the adsorbed PSC and the NADH in the solution. The probability of a side reaction occurring when one PSC molecule oxidizes one NADH is on the average 1/1100, as indicated by the data of Table I. When the side reaction takes place, part of the electrode surface is blocked from participating in further catalytic oxidation. Since the cross section of one NADH (2×10^{-14} cm^2) is approximately four times[31] that of a PSCH2 molecule (0.6×10^{-14} cm^2), several adsorbed mediators will become unavailable for NADH catalysis when a NADH molecule is coupled to the surface as illustrated in Figure 11. However, the mediators which are screened from reaction with solution NADH are still electroactive, as evidenced by the *i–E* wave on a scan in a buffer solution. This explains why a modified electrode, after scanning in a NADH solution, shows catalytic decay in spite of the fact that the coverage appears to be sufficient for a maximum current.

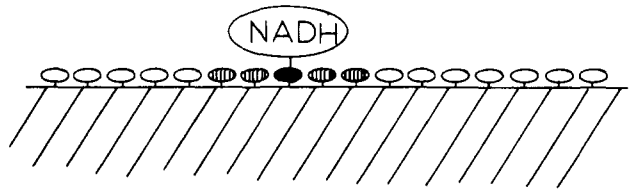

Figure 11. The figure is a model depicting how the electrochemically active mediators adsorbed on the electrode (striped ellipses) are blocked from the solution by the bulky NADH molecule after the chemical coupling reaction between the quinone and NADH has occurred. Only the mediator chemically coupled to the NADH molecule is electrochemically inactivated (closed ellipse). The open ellipses represent mediators still available for catalysis.

Table II[a]

electrode	NTC	NTC/M	PDCC	(NTC/M − PDCC)	no. of scans
1	551	0.51	0.47	0.04	5
2	518	0.48	0.52	−0.04	10
3	713	0.66	0.68	−0.02	30
4	536	0.49	0.58	−0.09	30
5	353	0.32	0.44	−0.12	30
6	188	0.17	0.21	−0.04	30
7	142	0.13	0.09	0.04	30

[a] NTC = number of turnovers of NADH per adsorbed mediator. NTC/M = NTC divided by the number of NADH oxidations per mediator necessary to deactivate one of them. See Table I, column ΣNADH/$\Delta\theta$. PDCC = percent decrease of catalytic current for the total number of scans in a NADH solution; see Figure 9.

The difference in stability for electrodes with varying coverages can be explained by the fact that an electrode with low coverage turns over a significantly larger number of NADH molecules per adsorbed mediator than an electrode with a high coverage. As a consequence, the probability for a side reaction is much greater.

Table II gives the total number of oxidized NADH molecules turned over by the adsorbed PSCH2. Obviously, the numbers of turnovers vs. coverage decreases with increasing coverage, thereby making the probability for a side reaction to occur much smaller. Table II also gives the probability for side reaction (NTC/M) and, hence, the average number of oxidations necessary for deactivation to occur. The percent decrease in the cataltyic current vs. the total number of scans (Figure 9) is given as PDCC. The conspicuous compatibility between the probability, NTC/M, and the percent decrease, PDCC, strongly suggests that there is a correlation between the fraction of mediators deactivated and the fraction of catalytic current lost. This correlation may be explained by a model in which the surface area of the electrode is divided into a discrete number of sites; each is the size of one NADH cross section. Every time a NADH molecule is coupled to a mediator on the surface, one of these sites is no longer available for catalysis. The larger the number of coupled NADH molecules, the greater is the area that is no longer available for catalysis. This model also infers that, at each NADH site in which blockage has occurred, no more coupling reactions can take place. This means that only one mediator, on the average, per NADH cross section is deactivated. This one-to-one correlation would account for the compatibility between the probability NTC/M and the percent decrease (PDCC) given in Table II.

As discussed in "Cataltic Stability", the apparent stability seemed to be better for electrodes with coverages higher than 1×10^{-9} mol/cm^2. It was also concluded in "Number of Layers"

(30) Moiroux, J.; Elving, P. J. *Anal. Chem.* **1978**, *50*, 1056–62.
(31) Dryhurst, G. "Electrochemistry of Biological Molecules"; Academic Press: New York, 1977.

that coverages greater than this corresponded to more than a monolayer. On the other hand, the data in Table II and Figure 10 suggest that the number of NADH oxidations per mediator necessary for a side reaction to take place decreases from 1100 to below 600, actually indicating a less stable electrode. This seemingly contradictory behavior is quite compatible with the blocking mechanism proposed above.

As two or three layers build up, the strength of adsorption for these layers decreases compared with mediators adsorbed directly to the surface. The strength of adsorption is decreased to such a degree that the PSC–NADH complex is no longer retained on the surface of the electrode, but is lost to the solution. This behavior is consistent with the data presented in Figure 2. The figure shows that there is virtually no change in $\Delta E_{p/2}$ for the multilayer coverages, whereas the submonolayer-covered electrodes showed significantly broader peaks. The broader peaks are evidence for stronger interactions between the different species on the surface of the electrode.[16] However, as more mediators per unit area are made available for catalysis, they are also made available for side reactions. Thus, the accumulated possibility for a side reaction per unit NADH site increases, since the protective cover of the complex is desorbed, leading to an apparently lower number of oxidations necessary for a side reaction to occur.

Coupling Reaction. When a PSCH2-modified electrode ($\Gamma = 0.7 \times 10^{-9}$ mol/cm^2) was scanned several times in a 2.0 mM NAD^+ solution prior to scanning in a 2.0 mM NADH solution, there were no adverse effects on the catalytic current. Thus, no part of the NAD^+ species reacts or couples to the oxidized mediator, so the coupling reaction with NADH must be a consequence of the detailed interaction between PCS and NADH in the chemical reaction mechanism.

It has been proposed, using direct electrochemical methods,[3,32] that the direct oxidation of NADH at solid electrodes proceeds according to the mechanism:

$$\mathrm{NADH} \xrightarrow{-e} \mathrm{NAD{\cdot}H^+} \xrightarrow{-H^+} \mathrm{NAD{\cdot}} \rightleftharpoons^{-e} \mathrm{NAD^+} \quad (12)$$

where $NAD{\cdot}H^+$ and NAD· are intermediate radicals in an ECE mechanism. Homogeneous disproportionation between the two radical species has been also proposed. Optical methods used in connection with electrochemical experiments also provided support for this reaction path.[33] It is therefore reasonable to assume that the detailed mechanism of the "catalytic" reaction between the mediator PSC and NADH involves radical species. A mechanism analogous to this was recently proposed by Miller et al.[34,35] in the catalytic oxidation of NADH through electrogenerated diimines. They suggested that the reaction with NADH proceeded by the rapid transfer of the 4-hydrogen in NADH to the oxidant, possibly in a stepwise fashion. It is probable that the only difference between the above two mechanisms is that, in the case of catalysis, there is a species present, namely, the quinone anion radical, which acts as a strong base; i.e., the proton is abstracted at a much faster rate than it is lost to the solution when no strong base is present. A probable reaction intermediate is, therefore, D, where the left

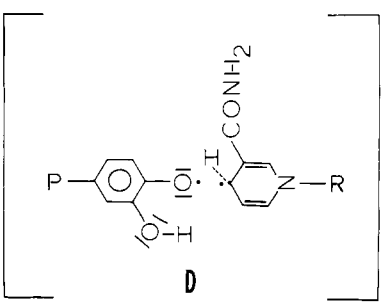

D

species is the semiquinone and the right one the NAD· radical, which has been documented[1] in the electrochemical reduction of NAD^+. In most cases the products in the next step are the catechol and the NAD^+, but statistically, once in 1100 oxidations (Table II), the product could be a complex such as E. This molecule

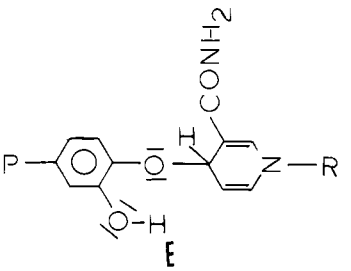

E

would account for a PSC–NADH species that poisons and "blocks off" the surface of the catalytic electrode. This species would also explain the loss of electroactivity in the adsorbed PSCH2 molecule, observed after several oxidative cycles. The fact that the NAD· radical is prone to dimerize is well established in the literature.[36] A coupling reaction between the semiquinone radical and the NAD· radical is therefore reasonable.

As a consequence of the structure of the proposed complex between the quinone and NADH, it seems unlikely that "capping" of sites in the quinone, e.g., the 2, 5, and 6 position by methyl groups, would have any significant effect on the blocking reaction.[23] It is therefore concluded that the catechol group probably does not offer the possibility of producing a stable catalytic electrode for NADH oxidation. Other mediators immobilized on carbon surfaces may provide a means of solving this problem.[37,38]

Experimental Section

Syntheses. 4-[2-(1-Pyrenyl)vinyl]catechol (pyrene–stilbene–catechol = PSCH2) and 4-[2-(1-pyrenyl)ethano]catechol (pyrene–ethano–catechol = PECH2) were synthesized in a series of steps.

1. 3,4-Methylenedioxybenzyl chloride was obtained by adding slowly, while stirring, 6.55 g of 3,4-methylenedioxybenzyl alcohol to a solution of dry ether mixed with 10.8 g of PCl_5 and 4.3 g of $CaCO_3$. The temperature was kept at 0 °C for 10 min, after which the solution was carefully washed several times with ice-cold[39] saturated Na_2CO_3. The ether phase was then dried with anhydrous $MgSO_4$ while stirring for several hours, after which the ether phase was evaporated. The residual 7.3 g was identified by IR spectroscopy and not further purified because of its high reactivity. The yield was nearly quantitative.

2. 3,4-Methylenedioxybenzyltriphenylphosphonium Chloride. A mixture of 7.3 g of 3,4-methylenedioxybenzyl chloride and 13.4 g of triphenylphosphine was refluxed at 140 °C while gently stirring in dry xylene for 24 h.[40] The white crystalline precipitate was filtered off and washed first with cold xylene and then with petroleum ether (boiling range 40–60 °C). The product, 13.9 g (yield 65%), was identified by IR and was not further purified.

3. 3,4-[2-(1-Pyrenyl)vinyl]methylenedioxybenzene. A mixture of 5.3 g of 1-pyrenecarboxaldehyde and 10.0 g of 3,4-methylenedioxybenzyltriphenylphosphonium chloride was dissolved in 100 mL of methylene chloride. To this solution was added 100 mL of $NaOH/H_2O$, 50/50 (w/w), during vigorous stirring.[41] After 25 min stirring was stopped and the reaction mixture poured into 0.5 L of ice water. After washing with another 0.5 L of water, the methylene chloride phase was separated and dried over anhydrous $MgSO_4$ for several hours. The triphenylphosphine oxide formed stoichiometrically was removed by adding 100 mL of ethanol (99.5%) and then the methylene chloride was evaporated off. The triphenylphosphine oxide remained dissolved in the resulting solution, while the 1-pyrene–stilbene–methylenedioxybenzene was precipitated quantitatively. The precipitate was analyzed with thin layer chromatography and found to consist of two species with a ΔR_f of 0.08. A

(32) Moiroux, J.; Elving, P. J. *J. Am. Chem. Soc.* **1980**, *102*, 6533–38.
(33) Pragst, F.; Kaltofen, B.; Volke, J.; Kuthan, J. *J. Electroanal. Chem.* **1981**, *119*, 301–14.
(34) Kitani, A.; Miller, L. *J. Am. Chem. Soc.* **1981**, *103*, 3595–97.
(35) Kitani, A.; So, Y. O.; Miller, L. *J. Electroanal. Chem.* **1981**, *103*, 7636–41.
(36) Jaegfeldt, H. *Bioelectrochem. Bioenerg.* **1981**, *8*, 355–70.
(37) Torstensson, A.; Gorton, L. *J. Electroanal. Chem.* **1981**, *130*, 199–207.
(38) Gorton, L.; Torstensson, A.; Johansson, G., private communication.
(39) Carman, R. M.; Shaw, I. M. *Aust. J. Chem.* **1976**, *29*, 133–43.
(40) Yamato, M.; Sato, K.; Hashigaki, K.; Koyama, T. *Chem. Pharm. Bull.* **1977**, *25*, 706–13.
(41) Märkl, G.; Mertz, A. *Synthesis* **1973**, *1*, 295–97.

mixture of 25/75 CH_2Cl_2/petroleum ether (40–60 °C) was used as eluent on silica gel thin layer plates. IR spectroscopy showed only the presence of the stilbene species, but NMR indicated that a 50/50% mixture of the cis and trans forms were present. The trans was separated quantitatively from the cis by first adding 25 mL of CH_2Cl_2 and then, while slowly stirring, petroleum ether. After 24 h at +4 °C, greenish yellow, slightly fluorescent, needle-like crystals were filtered off. Thin layer chromatography showed the presence of only one species, which was identified by NMR as the trans form. The yield of the trans form was 2.5 g which corresponds to 31%. The total yield of cis and trans was 5.5 g which corresponds to 68%. Only the trans form was used for further synthesis. Anal. Calcd: C, 86.2; H, 4.6; O, 9.2. Found: C, 86.5; H, 4.5; O, 8.8.

4. 4-[2-(1-Pyrenyl)vinyl]catechol. 3,4-[2-(1-Pyrenyl)vinyl]-methylenedioxybenzene (1.0 g) was dissolved in 75 mL of dry CH_2Cl_2 in a nitrogen atmosphere. Through a septum with the use of a syringe, 0.5 mL of 1.0 M BBr_3 dissolved in hexane was added. The temperature was kept below −65 °C with an ethanol–dry ice bath. After 30 min the reaction mixture was poured into a 1.0-L solution of water and ice. Nitrogen was bubbled continuously through the water–ice bath for another 30 min while stirring. The methylene chloride phase was extracted and dried with anhydrous $MgSO_4$. In the drying process the $MgSO_4$ became strongly colored, probably because of adsorption of polymeric products formed in the reaction.[42] The described procedure varied slightly from the one proposed by Eisenbaum et al.[43] in the cleavage of aryl methyl ethers. After drying, the solvent was evaporated until only 20 mL remained, after which 20 mL of petroleum ether was added. The solution was cooled down to −30 °C and a black undefined precipitate was filtered off. The temperature was lowered to −50 °C where bright yellow flakes started to precipitate. These flakes were filtered and dried in a vacuum dessicator for 18 h during which the powder turned slightly green. The powder was then stored in a dry nitrogen atmosphere. The product was identified as the desired product by mass spectroscopy; recovered amount was 0.6 g, yield 62%. A better yield might have resulted from using BCl_3 instead of[44] BBr_3. Anal. Calcd: C, 85.7; H, 4.8; O, 9.5. Found: C, 85; H, 4.7; O, 9.6.

5. 3,4-[2-(1-Pyrenyl)ethano]methylenedioxybenzene was synthesized from 3,4-[2-(1-pyrenyl)vinyl]methylenedioxybenzene by hydrogenation. The vinyl compound (1.0 g) was dissolved in 50 mL of ethyl acetate. To this solution was added 0.20 g of 10% Pd on activated carbon, and hydrogen at a pressure of 1 atm was applied.[45] When the reaction was stopped after 24 h of agitation, several spoons of Celite Filter Aid were added to the mixture in order to be able to filter off the Pd catalyst without igniting the solvent. The remaining solution was completely colorless, as opposed to the original strongly fluorescent greenish yellow one. The solvent was then dried with $MgSO_4$ and evaporated. The recovered product, a white powder, was identified by IR and NMR. The yield was quantitative. Anal. Calcd: C, 85.7; H, 5.1; O 9.1. Found: C, 85.3; H, 5.2; O, 8.8.

6. 4-[2-(1-Pyrenyl)ethano]catechol was synthesized from 0.86 g of 3,4-[2-(1-pyrenyl)ethano]methylenedioxybenzene by treatment with BBr_3 as described in step 4 for the vinyl compound. After evaporation of the solvent (until only 20 mL remained), 70 mL of petroleum ether was added. The solution was stored at −15 °C overnight. A white powder was filtered off and stored in a dry nitrogen atmosphere. The compound was identified using IR spectroscopy. The spectrum matched closely the analogous vinyl compound. The recovered amount was 0.52 g, which corresponds to a yield of 63%. Anal. Calcd: C, 85.2; H, 5.3; O, 9.5. Found: C, 85.3; H, 5.4; O, 9.7.

HPLC Purification. When the two different catechols were analyzed using HPLC, small amounts of impurities were found. To avoid complications in the electrochemical experiments, HPLC was used to produce the highly purified solutions from which the compounds were adsorbed. The chromatograph was a Chromatronix 3100. A head pressure of 1400 psi was applied from a nitrogen cylinder. For the HPLC separation, the catechols were dissolved in CH_2Cl_2/EtOH mixtures. Typically 100 μL of the catechol solutions was injected onto the column (Hypersil-5 μM ODS-C18, length 25 cm, i.d. 5 mm). The mobile phase used in the separations was a 88/12% mixture of ethanol and water. A few hundred microliters of the purified compounds was collected at the exit of the UV detector, at a time coinciding with the chromatographic peak maximum. The solution was then stored at −15 °C or used immediately.

Electrodes. The electrodes were spectrographic graphite rods, 6.0 mm o.d. (RW 003 Ringsdorff-Werke, GMBH). They were polished with emery paper (Tufbak Durite Waterproof Proof Closecote 600-A Type 1) which was placed on a rotating-disk polishing machine. The polishing was performed under a continuous flow of deionized water until the end of the rod was completely flat. The electrodes were typically 3 cm long and all were cut from the same graphite rod in order to avoid batch variations. Before mounting the electrodes in the holder for the electrochemical experiment, a heat-shrinkable polyethylene tube with a wall thickness of 0.1 mm was slipped over the rod in order to avoid electrical contact between the sides of the electrodes and the solution. This was done from the end opposite the polished surface to avoid affecting it mechanically or chemically. The edge of the tube was in-line with the electrode surface. The electrochemical surface area was identical with the geometric one when measured in a 2.0 mM ferrocyanide solution. The polyethylene tube as well as the sides of the electrode were quite hydrophobic, and no creeping of solution between the electrode and the polyethylene tube was observed.

Measurements. A triangular wave with linear ramp produced by an operational amplified circuit was fed to a three-electrode potentiostat, and the cyclic voltammograms were recorded on a Houston XY recorder, Model 2000. The reference electrode was a saturated calomel electrode, SCE, Radiometer K-401, and the auxilliary electrode was a Pt wire chemically isolated from the bulk of the solution with a glass frit. All measurements were made in buffers made from 0.10 M pyrophosphate (pH 4.0, 5.0, 6.0, 7.0, 8.0, and 9.0) or 0.10 M phosphate (pH 2.0, 3.0, 10.0, and 11.0). Measurements of areas on the chart paper, corresponding to a quantity of electrical charge, were made with a planimeter equipped with a magnifying glass (Gelman Instrument Co.). The uncertainty in charge was estimated as ±2%.

Adsorption Procedure. The electrodes were modified with 4-[2-(1-pyrenyl)vinyl]catechol or 4-[2-(1-pyrenyl)ethano]catechol by dipping them into a solution which had a concentration of approximately 0.05 mM of either compound. The solutions were slowly stirred during the adsorption process. By varying the time an electrode was in contact with the solution containing the electroactive species from 1 to 25 min, the coverage could be controlled from 0.10×10^{-9} to 3×10^{-9} mol/cm^2. An upper limit of 4×10^{-9} mol/cm^2 was reached even when the compounds were adsorbed from a more concentrated solution. When the electrodes were removed from the solution in which the adsorption took place, they were immediately washed with a jet of deionized water for at least 1 min.

A rubber tube used in an earlier work[14] in which 4-[2-(2-naphthyl)-vinyl]catechol was adsorbed in a similar manner was found to be unsuitable. The compounds used in this work were quite soluble in the rubber, and the thick walls (1.3 mm) quickly adsorbed them. Therefore, the much thinner polyethylene tube mentioned above was used. Care was still taken not to dip the tube-covered electrode into the solution containing the catechols any deeper than absolutely necessary.

Acknowledgment. The authors thank Dr. C. Ueda for valuable discussions during the course of this work and Dr. J. Lyga and Dr. T. Ingler for useful ideas in the synthetic work. The authors also want to thank Dr. Charles Miller for taking the electron microscope pictures of the spectrographic graphite. Financial support is gratefully acknowledged from Kemiska Institutionen, University of Lund, Knut and Alice Wallenbergs Stiftelse, Stiftelsen Bengt Lundquists Minne (Sweden), and the National Institutes of Health (USA), Grant No. NIH GM 19181.

Appendix

The integration of the differential equation A-1 (corresponds to eq 2) describing the surface reactions

$$QH_2 \overset{\text{rev.}}{\rightleftharpoons} Q \xrightarrow{k_b} \text{products}$$

$$QH_2 + Q \xrightarrow{k_a} \text{products}$$

is straightforward

$$-d\Gamma/dt = k_a[QH_2][Q] + k_b[Q]^2 \qquad \text{(A-1)}$$

Assuming reversible electrochemistry, i.e.

$$Q + 2H^+ + 2e^- \rightleftarrows QH_2$$

implies

$$E = E^{0'} - \frac{RT}{2F} \ln \frac{[QH_2]}{[Q]}$$

(42) McOmie, J. F. W.; Watts, M. L.; West, D. E. *Tetrahedron* **1968**, *24*, 2289–92.
(43) Vickery, E. H.; Pahler, L. F.; Eisenbaum, E. J. *J. Org. Chem.* **1979**, *44*, 4444–46.
(44) Gerecke, M.; Barer, R.; Brossi, A. *Helv. Chim. Acta* **1976**, *59*, 2551–57.
(45) Reiman, E. *Chem. Ber.* **1969**, *102*, 2881–88.

($E^{0'}$ contains the ln $[H^+]$ term) if and only if

$$\frac{[QH_2]}{[Q]} = \exp(E^{0'} - E)\frac{2F}{RT} = B(E) \qquad \text{(A-2)}$$

It is also assumed that

$$\begin{aligned} \Gamma_0 &= [QH_2]_0 + [Q]_0;\ t = 0 \\ \Gamma &= [QH_2] + [Q];\ t > 0 \end{aligned} \qquad \text{(A-3)}$$

"Eliminating" $[QH_2]$ from eq A-1 using eq A-2 implies

$$-d\Gamma/dt = k_a[Q]^2B(E) + k_b[Q]^2 \qquad \text{(A-4)}$$

if and only if

$$-d\Gamma/dt = (k_aB(E) + k_b)[Q]^2 \qquad \text{(A-5)}$$

From eq A-2 and A-3 it follows

$$\Gamma = (1 + B(E))[Q] \Leftrightarrow [Q] = \Gamma/(1 + B(E))$$

"Eliminating" $[Q]^2$ from eq A-5 implies

$$-\frac{d\Gamma}{dt} = (k_aB(E) + k_b)\frac{\Gamma^2}{(1 + B(E))^2} \qquad \text{(A-6)}$$

if and only if

$$-\frac{d\Gamma}{\Gamma^2} = \frac{(k_aB(E) + k_b)}{(1 + B(E))^2}\,dt \qquad \text{(A-7)}$$

Integration yields

$$\text{(left side)} - \int_{\Gamma_0}^{\Gamma}\frac{d\Gamma}{\Gamma^2} = -\left[-\frac{1}{\Gamma}\right]_{\Gamma_0}^{\Gamma} = \frac{1}{\Gamma} - \frac{1}{\Gamma_0} \qquad \text{(A-8)}$$

$$\text{(right side)}\ \frac{(k_aB(E) + k_b)}{(1 + B(E))^2}\int_0^t dt = \frac{(k_aB(E) + k_b)}{(1 + B(E))^2}t \qquad \text{(A-9)}$$

implying

$$\left(\frac{1}{\Gamma} - \frac{1}{\Gamma_0}\right) = \frac{(k_aB(E) + k_b)}{(1 + B(E))^2}t \qquad \text{(A-10)}$$

which is eq 3.

Registry No. PSCH2, 84432-98-4; PECH2, 84432-99-5; NADH, 58-68-4; graphite, 7782-42-5; 3,4-methylenedioxybenzyl chloride, 20850-43-5; triphenylphosphine, 603-35-0; 3,4-methylenedioxybenzyltriphenylphosphonium chloride, 63368-35-4; 1-pyrenecarboxaldehyde, 3029-19-4; (*E*)-3,4-[2-(1-pyranyl)vinyl]methylenedioxybenzene, 84433-00-1; 3,4-[2-(1-pyrenyl)ethano]methylenedioxybenzene, 84433-01-2; 3,4-methylenedioxybenzyl alcohol, 495-76-1; oxidized PSCH2, 84433-02-3; oxidized PECH2, 84433-03-4.

Solvation of Hydrogen Ions in Mixed Water–Alcohol Ion Clusters

A. J. Stace* and C. Moore

Contribution from the Department of Chemistry, The University, Southampton, Hants. S09 5NH, U.K. *Received June 14, 1982*

Abstract: From a study of the competitive decomposition processes of mixed ion clusters of the type $\{(ROH)_n\cdot(H_2O)_m\}H^+$ for $n + m < 20$, it has been possible to determine which of the species present in the cluster preferentially solvates the proton. The experiments have been performed on the following alcohols: propan-1-ol, propan-2-ol, butan-1-ol, 2-fluoroethanol, and 2-chloroethanol. In each case the occurrence of either alcohol or water loss from the ion clusters has been monitored as a function of n and m. Results for $\{(ROH)_n\cdot H_2O\}H^+$ show that in small clusters the alcohol molecules preferentially solvate the proton, but as the size of the cluster increases so the preference changes in favor of water. The value of n for which this transition occurs appears to depend upon the nature of the alcohol concerned. RRKM calculations have been used to investigate those features of the ion clusters which might be responsible for the observed transition in solvent preference. In particular, it is found that at least one of the reaction critical energies has to decrease as n increases, and that at some stage there has to be a transition in the relative magnitudes of the two critical energies. Two models are proposed to account for the experimental observations, and for each it is assumed that the solvent molecules are attached to a central stable nucleus of the form $(ROH)_3H^+$.

Introduction

In a recent publication,[1] results were presented in which the competitive solvation of hydrogen ions in mixed clusters of the type $\{(ROH)_n\cdot(H_2O)_m\}H^+$, had been studied as a function of cluster size for ROH equal to either methanol or ethanol. Although the results could be interpreted in terms of ion–dipole and ion–induced dipole interactions, it was only possible to produce a qualitative picture of intermolecular bonding within the ion clusters. The purposes of this paper are to present new experimental data which have been obtained by using alcohols with different molecular properties to those considered previously and to present the results of a series of calculations with which an attempt has been made to develop a more quantitative understanding of the bonding processes within mixed clusters of the above type. As before,[1] our objective in this work is to contribute toward a microscopic understanding of those interactions that exist between an ion and one or more solvent molecules. The study of ion clusters in the gas phase provides us with an opportunity to examine ions at varying stages of the solvation process without interference from the bulk solvent.[2-5]

The interpretation of our previous work[1] took into account those ion–dipole and ion–induced dipole interactions that it might be assumed are present in an ion cluster. It is obvious that this represents an oversimplification and that a detailed description of ion solvation is very much more complicated.[6] In addition to

(1) Stace, A. J.; Shukla, A. K. *J. Am. Chem. Soc.* **1982**, *104*, 5314.

(2) Kebarle, P. In "Ion-Molecule Reactions"; Franklin, J. L., Ed., Plenum Press: New York, 1972.
(3) Kebarle, P. *Ann. Rev. Phys. Chem.* **1977**, *28*, 445.
(4) Castleman, A. W., Jr. In "Kinetics of Ion–Molecule Reactions"; Ausloos, P. W., Ed.; Plenum Press: New York, 1979.
(5) Castleman, A. W., Jr. *Adv. Colloid Interface Sci.* **1979**, *10*, 73.
(6) Conway, B. E. "Ionic Hydration in Chemistry and Biophysics"; Elsevier: New York, 1981.

0002-7863/83/1505-1814$01.50/0